



Lung Ultrasound Score as a Predictor of Mortality in Patients With COVID-19

Zhenxing Sun^{1,2†}, Ziming Zhang^{1,2†}, Jie Liu^{1,2†}, Yue Song^{1,2}, Shi Qiao^{1,2}, Yilian Duan^{1,2}, Haiyan Cao^{1,2}, Yuji Xie^{1,2}, Rui Wang^{1,2}, Wen Zhang^{1,2}, Manjie You^{1,2}, Cheng Yu^{1,2}, Li Ji^{1,2}, Chunyan Cao^{1,2}, Jing Wang^{1,2}, Yali Yang^{1,2}, Qing Lv^{1,2}, Hongbo Wang^{3*‡}, Haotian Gu^{4*‡} and Mingxing Xie^{1,2*‡}

¹ Department of Ultrasound Medicine, Union Hospital, Tongji Medical College, Huazhong University of Science and Technology, Wuhan, China, ² Hubei Province Key Laboratory of Molecular Imaging, Wuhan, China, ³ Department of Gynecology and Obstetrics, Union Hospital, Tongji Medical College, Huazhong University of Science and Technology, Wuhan, China, ⁴ British Heart Foundation Centre of Research Excellence, King's College London, London, United Kingdom

OPEN ACCESS

Edited by:

Matteo Cameli,
University of Siena, Italy

Reviewed by:

Maria Concetta Pastore,
Università del Piemonte Orientale, Italy
Ciro Santoro,
Federico II University Hospital, Italy

*Correspondence:

Haotian Gu
haotian.gu@kcl.ac.uk
Hongbo Wang
drwanghb69@sina.com
Mingxing Xie
xiemx@hust.edu.cn

[†]These authors share first authorship

[‡]These authors share senior authorship

Specialty section:

This article was submitted to
Cardiovascular Imaging,
a section of the journal
Frontiers in Cardiovascular Medicine

Received: 25 November 2020

Accepted: 22 March 2021

Published: 25 May 2021

Citation:

Sun Z, Zhang Z, Liu J, Song Y, Qiao S, Duan Y, Cao H, Xie Y, Wang R, Zhang W, You M, Yu C, Ji L, Cao C, Wang J, Yang Y, Lv Q, Wang H, Gu H and Xie M (2021) Lung Ultrasound Score as a Predictor of Mortality in Patients With COVID-19. *Front. Cardiovasc. Med.* 8:633539. doi: 10.3389/fcvm.2021.633539

Background: Lung injury is a common condition among hospitalized patients with coronavirus disease 2019 (COVID-19). However, whether lung ultrasound (LUS) score predicts all-cause mortality in patients with COVID-19 is unknown. The aim of the present study was to explore the predictive value of lung ultrasound score for mortality in patients with COVID-19.

Methods: Patients with COVID-19 who underwent lung ultrasound were prospectively enrolled from three hospitals in Wuhan, China between February 2020 and March 2020. Demographic, clinical, and laboratory data were collected from digital patient records. Lung ultrasound scores were analyzed offline by two observers. Primary outcome was in-hospital mortality.

Results: Of the 402 patients, 318 (79.1%) had abnormal lung ultrasound. Compared with survivors ($n = 360$), non-survivors ($n = 42$) presented with more B2 lines, pleural line abnormalities, pulmonary consolidation, and pleural effusion (all $p < 0.05$). Moreover, non-survivors had higher global and anterolateral lung ultrasound score than survivors. In the receiver operating characteristic analysis, areas under the curve were 0.936 and 0.913 for global and anterolateral lung ultrasound score, respectively. A cutoff value of 15 for global lung ultrasound score had a sensitivity of 92.9% and specificity of 85.3%, and 9 for anterolateral score had a sensitivity of 88.1% and specificity of 83.3% for prediction of death. Kaplan–Meier analysis showed that both global and anterolateral scores were strong predictors of death (both $p < 0.001$). Multivariate Cox regression analysis showed that global lung ultrasound score was an independent predictor (hazard ratio, 1.08; 95% confidence interval, 1.01–1.16; $p = 0.03$) of death together with age, male sex, C-reactive protein, and creatine kinase-myocardial band.

Conclusion: Lung ultrasound score as a semiquantitative tool can be easily measured by bedside lung ultrasound. It is a powerful predictor of in-hospital mortality and may play a crucial role in risk stratification of patients with COVID-19.

Keywords: COVID-19, SARS-CoV-2, lung ultrasound score, mortality, prognosis

BACKGROUND

The coronavirus disease 2019 (COVID-19) is a newly recognized infectious disease caused by the severe acute respiratory syndrome coronavirus 2 (SARS-CoV-2). Although chest computed tomography (CT) has been regarded as an important diagnostic tool for COVID-19 diagnosis (1), it is limited by high cost, radiation exposure, infection control challenges, and lack of continuous monitoring, particularly for critically ill patients (2). Lung ultrasound (LUS), with the advantage of being non-invasive, low cost, and radiation free, has been increasingly used as a bed-side tool for evaluation and monitoring of lung diseases, particularly in the intensive care unit (ICU) (2, 3). It was found to have high accuracy in diagnosing viral community-acquired pneumonia with 94% sensitivity and 89% specificity for the detection of viral pneumonia in symptomatic patients (4). Global LUS score, a semiquantitative numerical score of lung aeration across 12 lung regions, has been shown as a useful tool to diagnose acute respiratory distress syndrome (ARDS) (5).

We therefore hypothesized that LUS score may play an important role in detecting lung lesions and optimizing risk stratification in patients with COVID-19. To test this hypothesis, LUS images in patients prospectively recruited from three hospitals in Wuhan, China were analyzed to evaluate the prognostic value of LUS score for in-hospital mortality in patients with COVID-19.

MATERIALS AND METHODS

Patient Population

Patients with confirmed COVID-19 who underwent lung ultrasound were consecutively recruited from the West Branch of Wuhan Union Hospital, Cancer Centre of Union Hospital, and Jiangnan Mobile Cabin Hospital Wuhan, China between February 6, 2020 and March 15, 2020. The study was approved by the ethics committee, Union Hospital, Tongji Medical College, Huazhong University of Science and Technology (No. 20200021). Written informed consent was waived because of the unprecedented nature of COVID-19 pandemic.

Inclusion criteria were age ≥ 18 years and confirmed COVID-19. Exclusion criteria were incomplete image acquisition, missing clinical data, and cardiac failure causing cardiogenic pulmonary oedema.

Demographic, clinical history, comorbidities, laboratory data, and outcomes of all patients were obtained from electronic medical records (Dthealth Medical Systems CO, Tianjin, China). Primary outcome was all-cause mortality. All patients were followed up until April 7, 2020 when the last patient in the study was discharged.

Lung Ultrasound

LUS examinations were performed by nine qualified ultrasound doctors using Mindray M9 portable ultrasound machines (Mindray Bio-medical electronics Co, Shenzhen, China) with 1- to 5- MHz convex probes. LUS consisted of 12 different regions (two anterior, two lateral, and two posterior thoracic regions) (**Supplementary Figure 1**) as previously described (6).

All video files were recorded in a hospital local archive and were interpreted and scored offline by two experienced observers within 24 h of LUS examinations who were blinded to the clinical data and outcomes. In case of disagreement between observers, the two observers agreed by consensus on the LUS score.

Examples of ultrasound findings including the patterns of B lines, consolidations, pleural line abnormalities, pleural effusion, and the lesion distribution are shown in **Figure 1**.

Lung Ultrasound Score

LUS score was determined based on four lung patterns (**Supplementary Table 1**): N = 0, B1 = 1, B2 = 2, and C = 3 as described previously (7):

- N pattern—normal aeration: A lines or < 3 isolated B lines;
- B1 pattern—moderate loss of lung aeration: a clear number of multiple visible B lines with horizontal spacing between adjacent B lines ≤ 7 mm (B1 lines);
- B2 pattern—severe loss of lung aeration: multiple B lines fused together with horizontal spacing between adjacent B lines ≤ 3 mm, including “white lung” (B2 lines); and
- C pattern—complete loss of aeration: pulmonary consolidation, presence of tissue pattern accompanied by static or dynamic air bronchograms.

Global LUS score was calculated by summing the scores of all 12 lung regions (ranging from 0 to 36). An adjusted composite score, antero-lateral score, was also derived by summing the anterior and lateral regional scores (range from 0 to 24) (5, 7).

Repeatability and Reproducibility of Lung Ultrasound Score

Intra- and interobserver variability of global LUS score was assessed in 30 randomly selected subjects by repeat measurements on the same images 1 month apart by two observers. Bland–Altman plots were produced.

Statistical Analysis

Demographic, clinical, and outcome variables were presented as percentages for categorical variables and as medians with interquartile ranges (IQRs) for continuous variables. The Mann–Whitney *U*-test was used to compare LUS scores between survivors and non-survivors.

Receiver operating characteristic (ROC) curves for death were drafted for global and anterolateral score. The area under the receiver operating characteristic curves (AUCs) was calculated to determine the diagnostic accuracy for death. The optimal cutoffs were determined as the highest Youden's index (sensitivity + specificity – 1).

Kaplan–Meier curves were used to examine cumulative death rate, and differences between groups were tested using a log rank test. Univariate and multivariate Cox regression analysis was performed to identify potential predictors of death. Multivariate models were constructed to assess the prognostic utility of global and anterolateral scores, incorporating covariables that were significant ($p < 0.05$) in the univariate analysis. All statistical analyses were performed using SPSS version 25 (SPSS Inc. Chicago, Illinois).

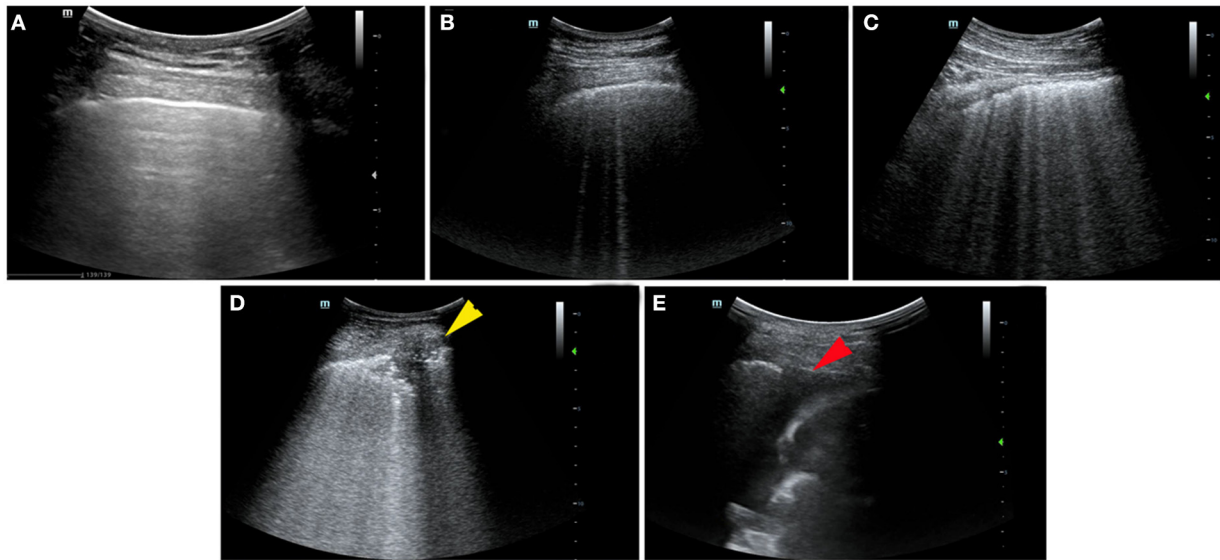


FIGURE 1 | Ultrasonographic features and lung ultrasound (LUS) score in patients with coronavirus disease 2019 (COVID-19). **(A)** Normal: the presence of A lines beyond the pleural line characterizes normal pulmonary aeration, LUS score: 0. **(B)** B1 line: the presence of multiple vertical B lines (comet tails) with well-defined spacing regularly spaced B lines 7 mm apart, LUS score: 1. **(C)** B2 line: the presence of coalescent B lines <3 mm apart, LUS score: 2. **(D)** Lung consolidation: the presence of a tissue pattern (yellow arrowhead), LUS score: 3. **(E)** Pleural effusion at costophrenic angle (red arrowhead).

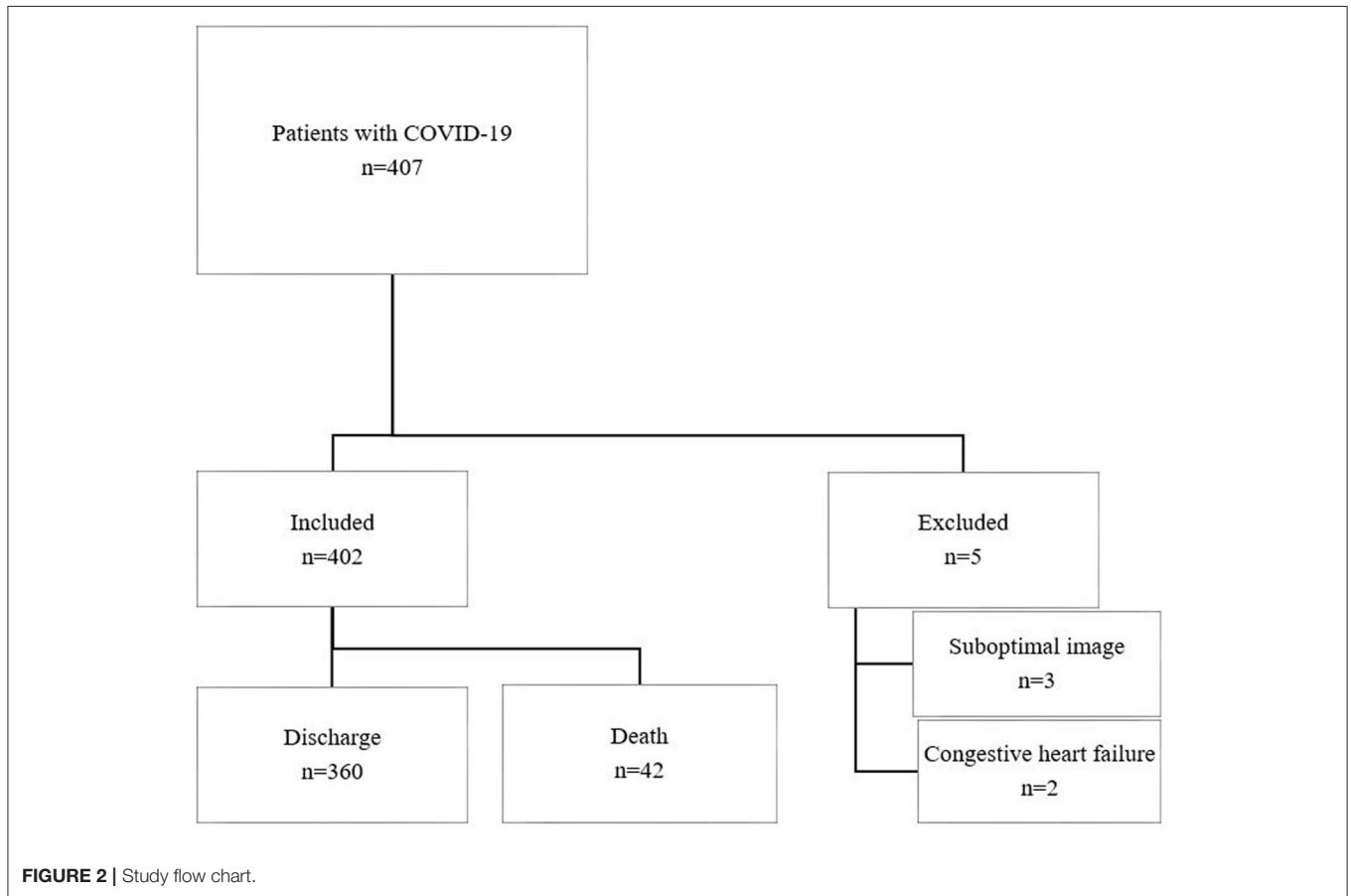


FIGURE 2 | Study flow chart.

TABLE 1 | Patient characteristics.

	No. (%)			p-value	No. (%)		p-value
	Total (N = 402)	Survivors (N = 360)	Non-survivors (N = 42)		Global LUS Score <15 (N = 310)	Global LUS Score ≥15 (N = 92)	
Age, median (IQR), years	63 (52–70)	62 (52–69)	69 (61–77)	<0.001	61 (51–68)	69 (61–77)	<0.001
Age distribution	–	–	–	<0.001	–	–	<0.001
20–40 years	39 (9.7)	39 (10.8)	0		36 (11.6)	4 (4.3)	
40–60 years	125 (31.1)	124 (34.5)	1 (2.4)		112 (36.1)	18 (19.6)	
≥60 years	238 (59.2)	197 (54.7)	41 (97.6)		162 (52.3)	70 (76.1)	
Sex	–	–	–	0.002	–	–	0.002
Female	210 (52.2)	199 (55.3)	11 (26.2)		175 (56.5)	35 (38.0)	
Male	192 (47.8)	161 (44.7)	31 (73.8)		135 (43.5)	57 (62.0)	
Clinical presentation							
Fever	395 (98.2)	353 (98.0)	42 (100)	0.36	304 (98.1)	91 (98.9)	0.93
Dry cough	279 (69.4)	246 (68.3)	33 (78.6)	0.17	209 (67.4)	70 (76.1)	0.11
Headache	23 (5.7)	18 (5.0)	5 (11.9)	0.14	14 (4.8)	9 (9.8)	0.06
Sore throat	45 (11.1)	42 (11.7)	3 (7.1)	0.53	31 (10.0)	14 (15.3)	0.16
Myalgia	135 (33.6)	116 (32.2)	19 (45.2)	0.09	97 (31.3)	38 (41.3)	0.07
Fatigue	131 (32.6)	115 (31.9)	16 (38.1)	0.42	100 (32.3)	31 (33.7)	0.80
Dyspnea	124 (30.8)	104 (23.2)	20 (34.8)	0.01	72 (23.2)	32 (34.8)	0.03
Rhinorrhea	43 (10.7)	35 (9.4)	8 (21.4)	0.11	32 (18.6)	11 (16.8)	0.66
Nausea and vomiting	26 (6.5)	24 (6.7)	2 (4.8)	0.89	23 (7.4)	3 (3.3)	0.15
Diarrhea	51 (12.7)	47 (13.1)	4 (9.5)	0.52	37 (11.9)	14 (15.2)	0.41
Comorbidities							
Hypertension	97 (24.1)	80 (22.2)	17 (40.5)	0.009	64 (20.6)	33 (35.9)	0.003
Coronary heart disease	50 (12.4)	35 (9.7)	15 (35.7)	<0.001	30 (9.7)	20 (21.7)	0.002
Arrhythmia	10 (2.5)	9 (2.5)	1 (2.4)	1.00	8 (2.6)	2 (2.2)	1.00
Diabetes	40 (10.0)	36 (10.0)	4 (9.5)	1.00	27 (8.7)	13 (14.1)	0.13
Cerebrovascular disease	12 (3.0)	9 (2.5)	3 (7.1)	0.23	6 (1.9)	6 (6.5)	0.06
Chronic pulmonary Disease	15 (3.7)	11 (3.1)	4 (9.5)	0.01	9 (2.9)	6 (6.5)	0.11
Chronic liver disease	17 (4.2)	15 (4.2)	2 (4.8)	1.00	12 (3.9)	5 (5.4)	0.72
Chronic kidney disease	5 (1.2)	4 (1.1)	1 (2.4)	1.00	3 (1.0)	2 (2.2)	0.70
Malignancy	25 (6.2)	18 (5.0)	7 (16.7)	0.009	14 (4.5)	11 (12.0)	0.01
Clinical outcome	–	–	–	<0.001	–	–	<0.001
Discharged	360 (89.6)	360 (100)	0		305 (98.4)	55 (59.8)	
Died	42 (10.4)	0	42 (100)		5 (1.6)	37 (40.2)	
ARDS	85 (21.1)	43 (11.9)	42 (100)	<0.001	17 (5.5)	68 (73.9)	<0.001
ICU admission	79 (19.7)	38 (10.5)	41 (97.6)	<0.001	15 (4.8)	64 (69.6)	<0.001
Mechanical Ventilation	76 (18.9)	36 (10.0)	40 (95.2)	<0.001	13 (4.2)	63 (68.5)	<0.001
Days from admission to ultrasonic examination, median (IQR), days	3 (2–5)	3 (2–5)	3 (1–4)	0.44	3 (2–5)	3 (2–5)	0.32
Length of hospital stay, median (IQR), days	27 (20–39)	28 (21–40)	23 (15–31)	0.002	27 (20–40)	27 (19–37)	0.88

Global LUS score: summing the scores of all 12 lung regions (two anterior, two lateral, and two posterior thoracic regions) (ranging from 0 to 36).

ARDS, acute respiratory distress syndrome; ICU, intensive care unit.

RESULTS

Patient Characteristics

A total of 407 patients with COVID-19 meeting the inclusion criteria were recruited, of whom 5 were excluded due to suboptimal LUS images ($n = 3$) and congestive heart failure ($n = 2$) (Figure 2). Four hundred two patients were included

in the final analysis, of whom 42 died with median time to death 21 (IQR, 14–29) days. Cause of death was recorded as multiorgan failure (42.9%), respiratory failure (26.1%), cardiac (9.5%), septic shock (9.5%), unknown (7.1%), and stroke (4.8%). Baseline characteristics are summarized in Table 1. Non-survivors were older and more male gender compared to survivors. There was a higher prevalence of

TABLE 2 | Laboratory findings.

	Median (IQR)			p-value	Median (IQR)		p-value
	Total (N = 402)	Survivors (N = 360)	Non-survivors (N = 42)		Global LUS Score <15 (N = 310)	Global LUS Score ≥15 (N = 92)	
Blood count							
WBC count, ×109/L	5.94 (4.73–7.56)	5.85 (4.62–6.87)	6.99 (4.98–10.51)	0.045	5.85 (4.62–6.87)	6.99 (4.98–10.51)	<0.001
Lymphocyte count, ×109/L	1.49 (1.11–1.87)	1.45 (1.09–1.85)	0.45 (0.28–0.78)	<0.001	1.60 (1.25–1.96)	0.97 (0.45–1.38)	<0.001
Platelet count, ×109/L	205 (160–250)	210 (167–255)	140 (92–208)	<0.001	211 (168–256)	179 (139–223)	<0.001
Hemoglobin, g/dl	120 (107–132)	121 (109–132)	104 (92–124)	0.001	122 (112–134)	107 (95–124)	<0.001
Coagulation function							
PT, s, (n = 384)	13.0 (12.4–13.8)	12.9 (12.4–13.6)	15.8 (13.9–18.4)	<0.001	12.9 (12.4–13.6)	13.8 (12.8–16.2)	<0.001
APTT, s, (n = 384)	37.1 (34.5–41.7)	36.7 (34.2–40.4)	47.9 (39.3–58.4)	<0.001	36.5 (34.2–40.3)	40.5 (35.1–49.5)	<0.001
D-dimer, mg/L, (n = 384)	0.44 (0.22–1.22)	0.39 (0.21–0.93)	3.08 (1.36–8.00)	<0.001	0.37 (0.20–0.84)	1.10 (0.39–3.01)	<0.001
Blood biochemistry							
TP, g/L	66.3 (62.7–70.2)	66.7 (63.5–70.6)	59.5 (54.8–65.4)	<0.001	66.7 (63.6–70.5)	64.3 (57.7–68.4)	0.003
Albumin, g/L	38.6 (35.0–41.5)	39.2 (36.3–41.8)	26.9 (24.4–30.1)	<0.001	39.6 (36.5–41.9)	33.7 (27.0–38.2)	<0.001
ALT, U/L	28 (19–47)	29 (19–46)	37.0 (22–70)	0.06	29.0 (19.5–46.0)	26.0 (18.0–47.0)	0.08
AST, U/L	24 (19–32)	23 (19.0–31)	42 (29–75)	0.01	23.0 (18.0–30.5)	31 (22.0–45.0)	0.02
TB, μmol/L	10.4 (7.8–13.7)	10.0 (7.7–13.1)	14.7 (9.5–28.8)	0.002	10.2 (7.8–13.2)	11.0 (7.5–15.4)	0.05
Sodium, mmol/L	139.8 (138.5–141.6)	139.7 (138.5–141.3)	141.5 (138.6–144.3)	0.05	139.8 (138.7–141.4)	139.8 (137.5–142.5)	0.98
Potassium, mmol/L	4.15 (3.90–4.37)	4.16 (3.93–4.37)	3.96 (3.55–4.39)	0.73	4.17 (3.94–4.37)	4.10 (3.79–4.40)	0.58
BUN, mmol/L, (n = 382)	4.92 (3.90–6.01)	4.75 (3.84–5.69)	10.61 (6.85–18.48)	<0.001	4.70 (3.87–5.70)	5.65 (4.23–10.52)	<0.001
Creatinine, μmol/L	64.3 (53.8–77.0)	63.8 (53.9–75.5)	76.9 (50.7–140.3)	0.024	63.5 (54.3–75.7)	68.7 (50.3–91.0)	0.05
hs-cTnI, pg/mL, (n = 382)	3.3 (1.7–12.1)	2.6 (1.6–6.5)	100.6 (29.3–407.4)	<0.001	2.50 (1.53–5.18)	15.4 (4.12–98.05)	<0.001
LDH, U/L	180 (153–228)	174 (151–206)	393 (278–670)	<0.001	174 (150–206)	216 (166–365)	0.001
CK-MB, U/L (n = 347)	0.9 (0.4–9.0)	0.8 (0.4–7.0)	21.6 (9.0–34.3)	0.008	0.8 (0.4–8.0)	1.9 (0.6–21.1)	0.03
Infection-related biomarkers							
CRP, mg/L, (n = 370)	3.03 (0.72–10.4)	2.43 (0.62–5.92)	90.19 (53.7–125.8)	<0.001	2.37 (0.59–5.8)	24.93 (2.21–105.6)	<0.001
PCT, ng/ml, (n = 370)	0.06 (0.04–0.13)	0.06 (0.04–0.11)	0.38 (0.14–1.51)	<0.001	0.06 (0.04–0.10)	0.07 (0.07–0.43)	0.03

WBC, white blood cell; PT, prothrombin time; APTT, activated partial thromboplastin time; TP, total protein; ALT, alanine transaminase; AST, aspartate aminotransferase; TB, total bilirubin; BUN, blood urea nitrogen; hs-cTnI, hypersensitive troponin I; LDH, lactate dehydrogenase; CK-MB, creatine kinase-MB; CRP, hypersensitive C-reactive protein; PCT, procalcitonin.

preexisting conditions including hypertension, coronary heart disease (CHD), and malignancy in non-survivors compared to survivors.

Laboratory Findings

Laboratory data on hospital admission are summarized in **Table 2**. Overall, non-survivors had significant worse

TABLE 3 | Lung ultrasound findings.

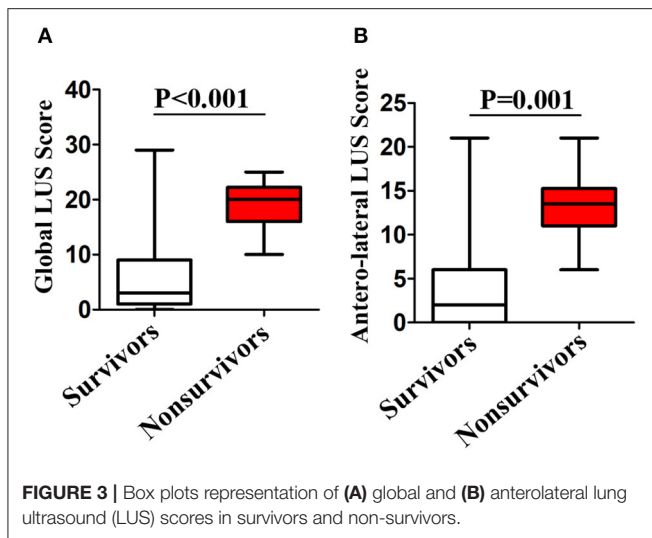
	No. (%)			p-value
	Total (N = 402)	Survivors (N = 360)	Non-survivors (N = 42)	
Normal baseline lung ultrasound	84 (20.9)	84 (23.3)	0	<0.001
Abnormal baseline lung ultrasound	318 (79.1)	276 (76.7)	42 (100)	
Characteristics of lung ultrasound				
B line	318 (79.1)	276 (76.7)	42 (100)	<0.001
B1 line	236 (58.7)	210 (58.3)	26 (61.9)	0.66
B2 line	213 (51.5)	171 (45.8)	42 (100)	<0.001
Pleural line abnormalities	137 (31.8)	103 (26.4)	34 (78.6)	<0.001
Pulmonary consolidation	117 (25.6)	83 (20.6)	34 (69.0)	<0.001
Pleural effusion	36 (8.2)	18 (4.4)	18 (40.5)	<0.001
Distribution at baseline ultrasound				<0.001
Right lung	63 (15.7)	63 (17.5)	0	
Left lung	30 (7.5)	30 (8.3)	0	
Bilateral lungs	223 (55.5)	181 (50.3)	42 (100)	
Abnormalities at lung region				
Left anterior superior	129 (32.1)	93 (25.8)	36 (85.7)	<0.001
Left anterior inferior	112 (28.4)	74 (20.6)	38 (90.5)	<0.001
Left lateral superior	128 (31.8)	100 (27.8)	28 (66.7)	<0.001
Left lateral inferior	153 (38.1)	112 (31.1)	41 (97.6)	<0.001
Left posterior superior	111 (27.6)	81 (22.5)	30 (71.4)	<0.001
Left posterior inferior	156 (38.8)	125 (34.7)	31 (73.8)	<0.001
Right anterior superior	139 (34.5)	108 (30.0)	31 (73.8)	<0.001
Right anterior inferior	138 (34.3)	102 (28.3)	36 (85.7)	<0.001
Right lateral superior	129 (32.1)	103 (28.6)	26 (61.9)	<0.001
Right lateral inferior	160 (39.8)	120 (33.3)	40 (95.2)	<0.001
Right posterior superior	142 (35.3)	107 (29.7)	35 (83.3)	<0.001
Right posterior inferior	150 (37.3)	130 (36.1)	20 (47.6)	0.14
Global LUS score, median (IQR)	4 (1–13)	3 (1–9)	20 (18–23)	<0.001
Anterolateral LUS score, median (IQR)	2 (0–8)	5 (0–9)	14 (11–15)	0.001

laboratory results, including increased white blood cell count, prothrombin time, activated partial thromboplastin time, D-dimer, aspartate aminotransferase, total bilirubin, blood urea nitrogen, creatinine, hypersensitive troponin I (hs-TnI), lactate dehydrogenase (LDH), creatine kinase–myocardial band (CK-MB), hypersensitive C-reactive protein (CRP), and procalcitonin and decreased lymphocyte count, platelet count, hemoglobin, total protein, and albumin (all $p < 0.05$) compared to survivors. Patients with a higher global LUS score (>15) had significant worse laboratory results, in particular, significantly increased D-dimer and CRP compared to those with a global LUS score <15 .

Lung Ultrasound Findings and Lung Ultrasound Score

Lung ultrasound was performed within a median of 3 (IQR, 2–5) days from hospital admission. Lung ultrasound findings are shown in **Table 3**. Eighty-four patients (20.9%)

had normal LUS. The presence of B lines was the most common finding (318/402, 79.1%), followed by pleural line abnormalities (137/402, 31.8%) and consolidation (117/402, 25.6%). Pleural effusions were detected in 36 (8.2%) patients. Compared to survivors, non-survivors were more likely to have B2 lines, pleural line abnormalities, pulmonary consolidation, and pleural effusion, but there was no difference in the presence of B1 lines. All non-survivors had bilateral involvement. Survivors had significantly lower global and anterior–lateral LUS scores compared to non-survivors (**Figure 3**). Findings of each of 12 lung regions are shown in **Supplementary Figure 2**. Regional LUS scores including anterior, lateral, and posterior scores are presented in **Supplementary Figure 3**. Bland–Altman plots for intra- and interobserver variability of global LUS score are shown in **Supplementary Figure 4**. All repeated measures were within $1.96 \times$ standard deviation of the mean, which suggested a good reproducibility of global LUS score.



Prediction of Mortality by LUS Global and Anterolateral Score

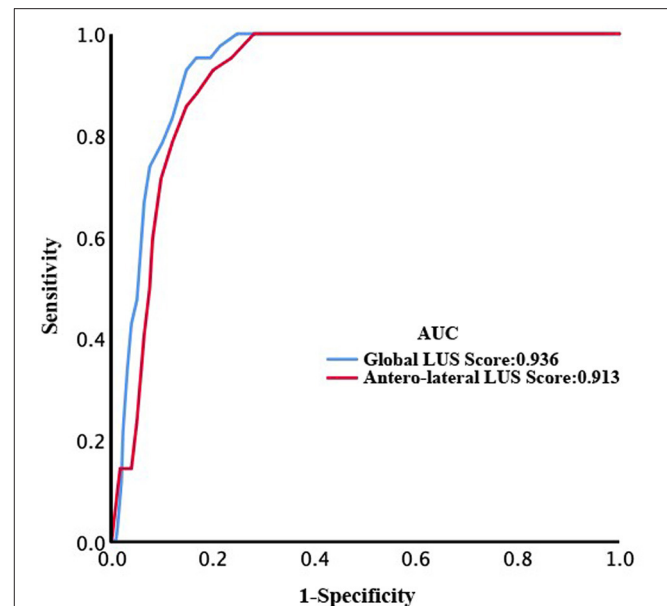
After a median of 27 (IQR, 20–39) days of follow-up, 42 patients died. ROC curve analyses of global and anterolateral LUS score for predicting mortality are shown in **Figure 4**. The area under the curve were 0.936 and 0.913 for global and anterolateral LUS score, respectively. A cutoff value of 15 for global LUS score had a sensitivity of 92.9% and specificity of 85.3% for prediction of death, and a cutoff value of 9 for anterolateral LUS score had a sensitivity of 88.1% and specificity of 83.3%. Clinical characteristics and laboratory findings dichotomized according to global LUS score optimal value of 15 are shown in **Tables 1, 2**.

Kaplan–Meier analysis showed that both global and anterolateral LUS scores were strong predictors of death (**Figure 5**). When global LUS score was >15 , 37/92 (40.2%) patients died compared to only 5/310 (1.6%) death in those with a global LUS score <15 . When patients were dichotomized by anterolateral LUS score of 9, there were 36/97 (37.1%) deaths in patients with a high score compared to 6/305 (2.0%) deaths in those with a low anterolateral score.

On univariate Cox regression analysis, age, male gender, malignancy, CHD, CRP, hs-cTnl, CK-MB, D-dimer, global LUS score, and anterolateral LUS score were significantly associated with mortality (**Table 4**). In multivariate model 1, considering global LUS score together with other significant predictors in the univariate model, age, male sex, CRP, CK-MB, and global LUS score [hazard ratio (HR), 1.08; 95%CI, 1.01–1.16, $p = 0.03$] remained as a significant predictor. In multivariate model 2, when anterolateral LUS score was tested with other variables, the predictive power of anterolateral LUS score did not remain significant.

DISCUSSION

Our data suggested that global LUS score was a predictor of in-hospital mortality independent of age, gender, comorbidities, and biochemical markers and was superior to LUS anterolateral



score. The optimal threshold of 15 for global LUS score and 9 for anterolateral LUS score were in line with those derived from previous investigations (5, 8). These findings supported the clinical utility of LUS in patients with COVID-19 (7, 9) given its ease of use at point of care, low cost, lack of radiation exposure, and ready combination with other components of critical care ultrasonography (10, 11).

LUS features in patients with COVID-19 in our study manifested as multiple lesions, various types of B lines, irregularly pleural lines, and subpleural consolidations. B lines presented in 79.1% patients. B2 lines and consolidations were more common in non-survivors than in survivors. Pleural effusion, pleural thickening, and pneumothorax were less common in COVID-19 patients, which were consistent with the latest autopsy report (12) that COVID-19 patients presented with acute interstitial lung disease.

Bass et al. showed that LUS had high sensitivity for detection of interstitial and alveolar–interstitial lung disease with peripheral distribution (13). Consistent with these features, our findings suggested that global LUS score was highly predictive of death in COVID-19 and independent of other previously identified predictors. Non-survivors in our study were older and more male with higher prevalence of preexisting conditions including hypertension, CHD, and malignancy and higher levels of cardiac injury and systematic inflammation markers than survivors, which were in consistency with previous studies (14).

Another interesting finding of our study was that when the posterior regions were excluded, the predictive power of anterolateral LUS score disappeared in the multivariate cox regression model. This finding was consistent with chest CT findings that the most commonly involved lung segments in patients with COVID-19 were the dorsal segment of the right

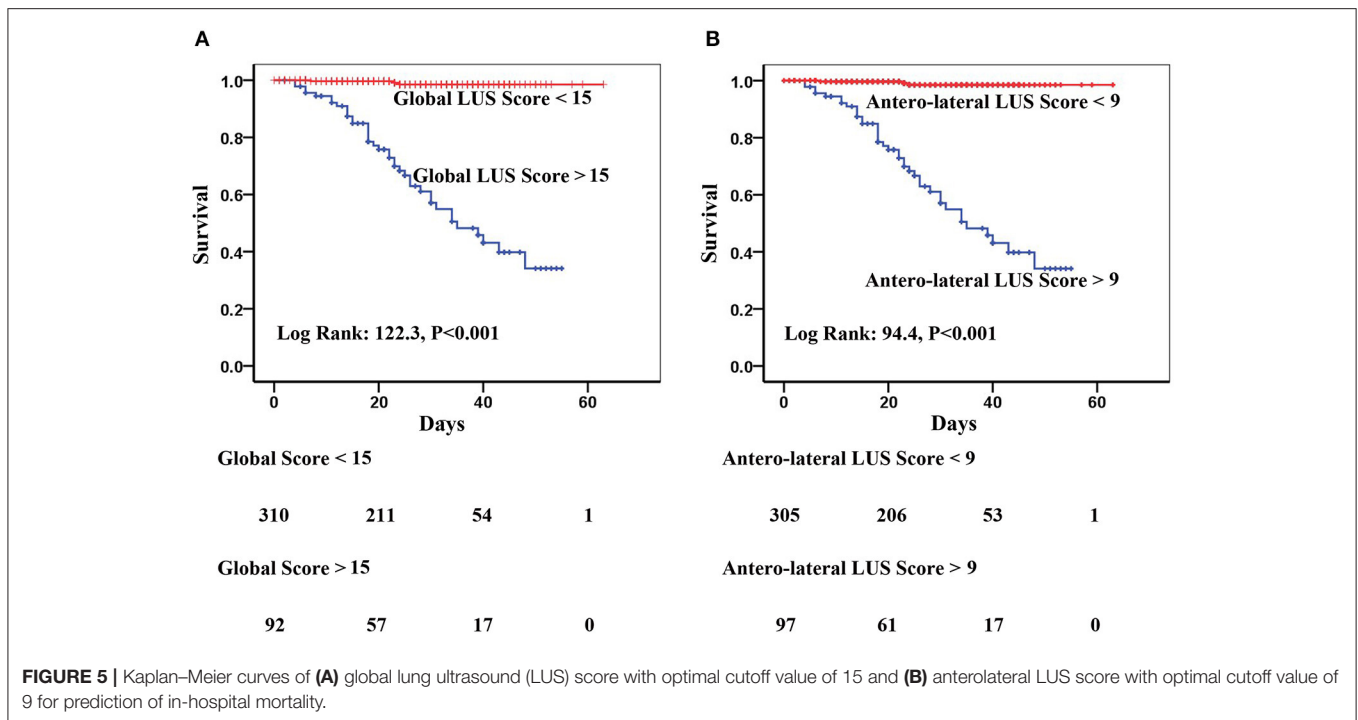


TABLE 4 | Univariate and multivariate Cox regression.

	HR	CI (95%)	p	HR	CI (95%)	p	HR	CI (95%)	p
	Univariate			Model 1			Model 2		
Age	1.04	1.01–1.07	0.005	1.05	1.00–1.10	0.04	1.05	1.00–1.09	0.05
Male sex	0.33	0.17–0.67	0.002	0.31	0.11–0.89	0.03	0.34	0.12–0.92	0.03
Hypertension	0.55	0.30–1.03	0.06						
Malignancy	0.32	0.14–0.72	0.006	0.57	0.18–1.81	0.34	0.57	0.18–1.82	0.34
CHD	0.28	0.15–0.52	<0.001	0.99	0.45–2.18	0.99	0.93	0.43–2.02	0.85
CRP	2.58	1.99–3.35	<0.001	1.60	1.17–2.20	0.004	1.69	1.23–2.31	0.001
hs-cTnl	1.82	1.61–2.04	<0.001	1.11	0.90–1.37	0.34	1.17	0.95–1.44	0.14
CK-MB	2.11	1.75–2.54	<0.001	1.47	1.09–1.99	0.01	1.54	1.13–2.08	0.006
D-Dimer	2.75	2.08–3.65	<0.001	1.19	0.83–1.69	0.34	1.17	0.82–1.66	0.38
Global LUS score	1.20	1.15–1.26	<0.001	1.08	1.01–1.16	0.03			
Anterolateral LUS score	1.23	1.17–1.29	<0.001				1.04	0.96–1.13	0.34
C-index				0.995			0.994		

CHD, coronary heart disease; CRP, C-reactive protein; hs-cTnl, hypersensitive troponin I; CK-MB, creatine kinase–myocardial band.

Global LUS score: summing the scores of all 12 lung regions (two anterior, two lateral, and two posterior thoracic regions) (ranging from 0 to 36). The values in bold represent statistical differences in data.

lower lobe, the posterior basal segment of the right lower lobe, the lateral basal segment of the right lower lobe, and the dorsal segment and the posterior basal segment of the left lower lobe (15). Despite some studies showing that the posterior regions had the lowest diagnostic accuracy (5), scores from these regions could play an important role in risk stratification. In the present study, lung lesions were mainly located in the right lateral inferior area (39.8%), left lateral inferior area (38.1%), left posterior inferior area (38.8%), and right posterior inferior area (37.3%) (the lower posterior and lateral segments of the lungs). This finding also supported that the potential benefit of prone position

in patients affected with COVID-19 acute respiratory distress syndrome (ARDS) due to a more even distribution of the gas–tissue ratios along the dependent–non-dependent axis and a more homogeneous distribution of lung stress and strain (16).

Although anterolateral LUS score had less predictive power compared to global LUS score, it may still play an important role particularly in patients on ICU.

Clinical Implications

COVID-19 as a global pandemic imposes a huge burden on medical systems. Early quantification of patients with severe lung

involvement may be critical for optimization of treatment and management. LUS as a non-invasive and cost-effective diagnostic tool can be performed rapidly, particularly in ICU. Severe studies have also demonstrated that echocardiography is a crucial tool in detecting cardiovascular complications (in particular on assessment of left and right ventricular function) and predicts poor prognosis in patients COVID-19 (17, 18). Combining LUS with echocardiography may add additional value to identify patients at higher risk of poor outcomes.

Limitations

Our study has several limitations. First, mortality rate was relatively low, which limits the strength of our conclusion. Low mortality rate may be due to the fact that majority of patients in the present study were not in ICU, while this rate was similar to previously published data (19). Second, the follow-up period was relatively short, as majority of patients were discharged within 28 days from admission.

Although our findings suggested that LUS may add additional value in risk stratification, the strength of our conclusion may be limited by the nature of an observational study. There are several other limitations of LUS that cannot be ignored such as the requirement of special training to perform high-quality LUS, lack of evidence-based guidelines, the high risk of infection when performing LUS examination in patients with COVID-19 (20, 21).

Patients included in this study were recruited from three hardest-hit hospitals in Wuhan, and these patients may not represent the population in other areas. Finally, the relationship between LUS and lung CT was not explored, as the majority of patients did not have lung CT due to limited availabilities and the nature of infectious disease.

CONCLUSION

Global LUS score as a semiquantitative measure of lung conditions is a powerful predictor of in-hospital mortality in patients with COVID-19 and may add additional value in patient monitoring and risk stratification.

DATA AVAILABILITY STATEMENT

The raw data supporting the conclusions of this article will be made available by the authors, without undue reservation.

REFERENCES

- Shi H, Han X, Jiang N, Cao Y, Alwalid O, Gu J, et al. Radiological findings from 81 patients with COVID-19 pneumonia in Wuhan, China: a descriptive study. *Lancet Infect Dis.* (2020) 20:425–34. doi: 10.1016/S1473-3099(20)30086-4
- Lepri G, Orlandi M, Lazzeri C, Bruni C, Hughes M, Bonizzoli M, et al. The emerging role of lung ultrasound in COVID-19 pneumonia. *Eur J Rheumatol.* (2020) 7:129–33. doi: 10.5152/eurjrheum.2020.2063
- Volpicelli G, Lamorte A, Villen T. What's new in lung ultrasound during the COVID-19 pandemic. *Intensive Care Med.* (2020) 46:1445–48. doi: 10.1007/s00134-020-06048-9

ETHICS STATEMENT

The studies involving human participants were reviewed and approved by Union Hospital, Tongji Medical College, Huazhong University of Science and Technology. Written informed consent for participation was not required for this study in accordance with the national legislation and the institutional requirements. Written informed consent was obtained from the individual(s) for the publication of any potentially identifiable images or data included in this article.

AUTHOR CONTRIBUTIONS

ZS, HW, HG, and MX conceived and designed the study. ZZ and JL contributed to the literature search. ZS, CC, SQ, YS, YD, WZ, MY, and LJ contributed to data collection. ZZ, CY, and HG contributed to data analysis. JW, YY, QL, and HG contributed to data interpretation. YX and RW contributed to the figures. ZS, HG, ZZ, and JL drafted the article. All authors contributed to the article and approved the submitted version.

FUNDING

We acknowledge the financial support from the National Natural Science Foundation of China (grant 81922033 to Li Zhang; grant 81727805 to MX; and grant 81701716 to ZS) and National Institute for Health Research, UK (ICA-CL-2018-04-ST2-012) to HG and by British Heart Foundation, UK (PG/19/23/34259) to HG.

ACKNOWLEDGMENTS

We are grateful for all our colleagues, especially Dr. Li Zhang and Hongliang Yuan, for their support to the present study. We are also grateful to the many frontline medical staffs for their dedication in the face of this outbreak despite the potential threat to their own lives and the lives of their families.

SUPPLEMENTARY MATERIAL

The Supplementary Material for this article can be found online at: <https://www.frontiersin.org/articles/10.3389/fcvm.2021.633539/full#supplementary-material>

- Zhang YK, Li J, Yang JP, Zhan Y, Chen J. Lung ultrasonography for the diagnosis of 11 patients with acute respiratory distress syndrome due to bird flu H7N9 infection. *Virology.* (2015) 12:176. doi: 10.1186/s12985-015-0406-1
- Pisani L, Vercesi V, van Tongeren PSI, Lagrand WK, Leopold SJ, Huson MAM, et al. The diagnostic accuracy for ARDS of global versus regional lung ultrasound scores - a post hoc analysis of an observational study in invasively ventilated ICU patients. *Intensive Care Med Exp.* (2019) 7:44. doi: 10.1186/s40635-019-0241-6
- Bouhemad B, Mongodi S, Via G, Rouquette I. Ultrasound for "lung monitoring" of ventilated patients. *Anesthesiology.* (2015) 122:437–47. doi: 10.1097/ALN.0000000000000558

7. Volpicelli G, Elbarbary M, Blaivas M, Lichtenstein DA, Mathis G, Kirkpatrick AW, et al. International evidence-based recommendations for point-of-care lung ultrasound. *Intensive Care Med.* (2012) 38:577–91. doi: 10.1007/s00134-012-2513-4
8. Tierney DM, Boland LL, Overgaard JD, Huelster JS, Jorgenson A, Normington JP, et al. Pulmonary ultrasound scoring system for intubated critically ill patients and its association with clinical metrics and mortality: a prospective cohort study. *J Clin Ultrasound.* (2018) 46:14–22. doi: 10.1002/jcu.22526
9. Nazerian P, Volpicelli G, Vanni S, Gigli C, Betti L, Bartolucci M, et al. Accuracy of lung ultrasound for the diagnosis of consolidations when compared to chest computed tomography. *Am J Emerg Med.* (2015) 33:620–5. doi: 10.1016/j.ajem.2015.01.035
10. Peng QY, Wang XT, Zhang LN. Findings of lung ultrasonography of novel corona virus pneumonia during the 2019-2020 epidemic. *Intensive Care Med.* (2020) 46:849–50. doi: 10.1007/s00134-020-05996-6
11. Vetrugno L, Bove T, Orso D, Barbariol F, Bassi F, Boero E, et al. Our Italian experience using lung ultrasound for identification, grading and serial follow-up of severity of lung involvement for management of patients with COVID-19. *Echocardiography.* (2020) 37:625–27. doi: 10.1111/echo.14664
12. Xu Z, Shi L, Wang Y, Zhang J, Huang L, Zhang C, et al. Pathological findings of COVID-19 associated with acute respiratory distress syndrome. *Lancet Respir Med.* (2020) 8:420–22. doi: 10.1016/S2213-2600(20)30076-X
13. Bass CM, Sajed DR, Adedipe AA, West TE. Pulmonary ultrasound and pulse oximetry versus chest radiography and arterial blood gas analysis for the diagnosis of acute respiratory distress syndrome: a pilot study. *Crit Care.* (2015) 19:282. doi: 10.1186/s13054-015-0995-5
14. Luo X, Zhou W, Yan X, Guo T, Wang B, Xia H, et al. Prognostic value of C-reactive protein in patients with COVID-19. *Clin Infect Dis.* (2020) 71:2174–9. doi: 10.1093/cid/ciaa641
15. Wu J, Wu X, Zeng W, Guo D, Fang Z, Chen L, et al. Chest CT findings in patients with coronavirus disease 2019 and its relationship with clinical features. *Invest Radiol.* (2020) 55:257–61. doi: 10.1097/RLI.0000000000000670
16. Guérin C, Albert RK, Beitler J, Gattinoni L, Jaber S, Marini JJ, et al. Prone position in ARDS patients: why, when, how and for whom. *Intensive Care Med.* (2020) 46:2385–96. doi: 10.1007/s00134-020-06306-w
17. Moody WE, Mahmoud-Elsayed HM, Senior J, Gul U, Khan-Kheil AM, Horne S, et al. Impact of right ventricular dysfunction on mortality in patients hospitalized with COVID-19, according to race. *CJC Open.* (2021) 3:91–100. doi: 10.1016/j.cjco.2020.09.016
18. Cameli M, Pastore MC, Soliman Aboumarie H, Mandoli GE, D'Ascenzi F, et al. Usefulness of echocardiography to detect cardiac involvement in COVID-19 patients. *Echocardiography.* (2020) 37:1278–86. doi: 10.1111/echo.14779
19. Chen N, Zhou M, Dong X, Qu J, Gong F, Han Y, et al. Epidemiological and clinical characteristics of 99 cases of 2019 novel coronavirus pneumonia in Wuhan, China: a descriptive study. *Lancet.* (2020) 395:507–13. doi: 10.1016/S0140-6736(20)30211-7
20. Gargani L, Soliman-Aboumarie H, Volpicelli G, Corradi F, Pastore MC, Cameli M. Why, when, and how to use lung ultrasound during the COVID-19 pandemic: enthusiasm and caution. *Eur Heart J Cardiovasc Imaging.* (2020) 21:941–8. doi: 10.1093/ehjci/jeaa163
21. Di Serafino M, Notaro M, Rea G, Iacobellis F, Delli Paoli V, Acampora C, et al. The lung ultrasound: facts or artifacts? In the era of COVID-19 outbreak. *Radiol Med.* (2020) 125:738–53. doi: 10.1007/s11547-020-01236-5

Conflict of Interest: The authors declare that the research was conducted in the absence of any commercial or financial relationships that could be construed as a potential conflict of interest.

Copyright © 2021 Sun, Zhang, Liu, Song, Qiao, Duan, Cao, Xie, Wang, Zhang, You, Yu, Ji, Cao, Wang, Yang, Lv, Wang, Gu and Xie. This is an open-access article distributed under the terms of the Creative Commons Attribution License (CC BY). The use, distribution or reproduction in other forums is permitted, provided the original author(s) and the copyright owner(s) are credited and that the original publication in this journal is cited, in accordance with accepted academic practice. No use, distribution or reproduction is permitted which does not comply with these terms.